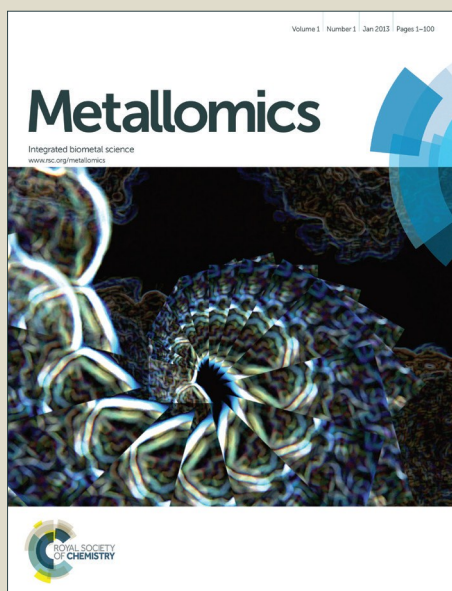


Metallomics

Accepted Manuscript



This is an *Accepted Manuscript*, which has been through the Royal Society of Chemistry peer review process and has been accepted for publication.

Accepted Manuscripts are published online shortly after acceptance, before technical editing, formatting and proof reading. Using this free service, authors can make their results available to the community, in citable form, before we publish the edited article. We will replace this *Accepted Manuscript* with the edited and formatted *Advance Article* as soon as it is available.

You can find more information about *Accepted Manuscripts* in the [Information for Authors](#).

Please note that technical editing may introduce minor changes to the text and/or graphics, which may alter content. The journal's standard [Terms & Conditions](#) and the [Ethical guidelines](#) still apply. In no event shall the Royal Society of Chemistry be held responsible for any errors or omissions in this *Accepted Manuscript* or any consequences arising from the use of any information it contains.

[Ru(phen)₂dppz]²⁺ (phen=1,10-phenanthroline, dppz=dipyrido [3,2-a:2'.3'-c] phenazine) holds red-shifted emission, large Stokes shifts about 190 nm and high photo-stability, which has been widely used to monitor protein aggregation and used to monitor in real-time the transition of Aβ₁₋₄₀ monomers into fibrils.^{16,17} As shown in Figure 1, Compound [Ru(phen)₂dppz]²⁺ itself showed very weak fluorescence emission (Fig.1a), which was significantly increased after mixed with Aβ₁₋₄₂ with Cu²⁺ ions (Fig.1b), suggesting high affinity of this compound for amyloidogenic Aβ₁₋₄₂ with Cu²⁺ aggregates. After addition of CeONP, the fluorescence intensity of [Ru(phen)₂dppz]²⁺ with Aβ₁₋₄₂ with Cu²⁺ ions was decreased 62% (Fig. 1c). These results further confirmed that CeONP can effectively reduce the amyloid peptide aggregation in vitro.

The effect of CeONP in inhibiting amyloid peptide from aggregation by photoluminescence of [Ru(phen)₂dppz]²⁺ was also detected in SH-SY5Y cells. External Aβ₁₋₄₂ could enter SH-SY5Y cells and aggregated in cytoplasm, which were confirmed by fluorescence microscopy images of SH-SY5Y cells stained with FITC-labeled Aβ₁₋₄₂(50μM, green) (Fig. S1) (FITC means fluorescein isothiocyanate isomer). We observed that FITC-labeled Aβ₁₋₄₂ aggregated around SH-SY5Y nuclei, which was stained with DAPI (blue). Aβ₁₋₄₂ or Aβ₁₋₄₂ plus Cu²⁺ was incubated with SH-SY5Y cells in the presence of [Ru(phen)₂dppz]²⁺. Photoluminescence properties of Aβ₁₋₄₂-treated SH-SY5Y cells were examined by confocal scanning laser microscopy. SH-SY5Y cells, after incubated with Aβ₁₋₄₂, displayed some red photoluminescence intensity of [Ru(phen)₂dppz]²⁺ (Fig. 2B), comparing with the control of SH-SY5Y cells alone (Fig. 2A). The treatment of SH-SY5Y cells with Aβ₁₋₄₂ plus Cu²⁺ resulted in dramatic increase in [Ru(phen)₂dppz]²⁺ photoluminescence intensity, suggesting the binding of [Ru(phen)₂dppz]²⁺ with aggregated amyloid peptide (Fig. 2C). These results indicated that Cu²⁺ ions induced tremendous Aβ₁₋₄₂ aggregation, and [Ru(phen)₂(dppz)]²⁺ interacted strongly with the fibril framework of the amyloid peptide, which changed the polarity of the microenvironment felt by the dppz ligand, favoring the luminescent state. However, in the presence of CeONP, the red [Ru(phen)₂dppz]²⁺ photoluminescence intensity of SH-SY5Y cells treated with Aβ₁₋₄₂ plus Cu²⁺ dramatically decreased (Fig. 2D). This study revealed that CeONP played a pivotal role in suppression of Aβ₁₋₄₂ aggregation.

In the presence or absence of CeONP, the aggregation extents and morphology of Aβ₁₋₄₂ plus Cu²⁺ were monitored by transmission electron microscopy (TEM) (Fig. S2).¹⁴ After 72 h of quiescent incubation at 37°C, Aβ₁₋₄₂ plus Cu²⁺ displayed abundance of cross-linked fibril aggregations (Fig. S2A). The aggregation fibrils of Aβ₁₋₄₂ induced by Cu²⁺ was obviously reduced after CeONP-treatment (Fig. S2B). The results, consistent with photoluminescence of Ru(phen)₂dppz]²⁺ study, suggested that CeONP decreased the aggregation tendency and intensity of Aβ₁₋₄₂.

The study by mass spectroscopy (Fig. S3) demonstrated that CeONP can effectively decrease Cu²⁺-induced Aβ₁₋₄₂ aggregation intensity. The mass spectrometry analysis indicated that Aβ₁₋₄₂

appeared at m/z = 1083. After addition of Cu²⁺ ions, peaks of amyloid peptides shifted to m/z = 1099, corresponding to more aggregated oligomer forms. Cu²⁺ ions promoted the processes of Aβ₁₋₄₂ aggregation. In the presence of CeONP, the oligomers of Aβ₁₋₄₂ with Cu²⁺ at m/z = 1099 shifted back to m/z = 1083. These peaks shift of Aβ₁₋₄₂ indicated that CeONP inhibits the aggregation of Aβ₁₋₄₂, despite it is difficult to quantitatively identify what kinds of Aβ₁₋₄₂ oligomers.

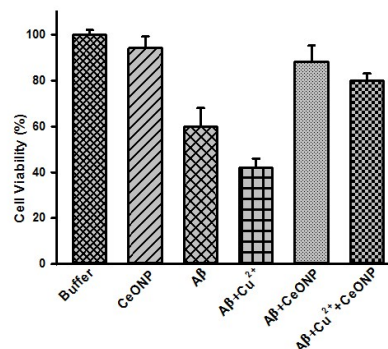


Figure 3. Cell viability of SH-SY5Y cells in different conditions. The cells were treated with 50 μM Aβ₁₋₄₂ or 50 μM Cu²⁺-Aβ₁₋₄₂ in the presence or absence of 50 μM CeONP.

To evaluate the role of CeONP on neuronal cytotoxicity of Aβ₁₋₄₂ plus Cu²⁺ ions, cell viability was determined quantitatively by MTT assay using SH-SY5Y human neuroblastoma cells. Aβ₁₋₄₂ in the oligomeric state is cytotoxic to neuronal cells.¹⁸ As Figure 3 shown, the cell viability was about 60% and 42%, when incubated the cells with Aβ₁₋₄₂ and Cu²⁺+Aβ₁₋₄₂, respectively. Upon treatment of the cells with CeONP, the cell viability was increased to 90% and 81%, with Aβ₁₋₄₂ and Cu²⁺+Aβ₁₋₄₂, respectively. The results indicated that CeONP can significantly protect against neuronal cytotoxicity from amyloid peptide and copper ions.

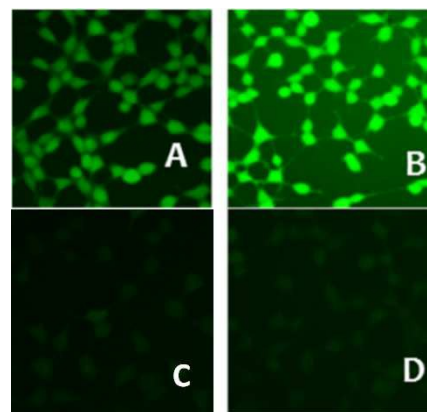


Figure 4. Fluorescence assays of ROS in living SH-SY5Y cells. The ROS was monitored by a fluorescent assay kit of DCFH. (A) Aβ₁₋₄₂; (B) Cu²⁺ + Aβ₁₋₄₂; (C) Aβ₁₋₄₂ + CeONP; (D) Cu²⁺ + Aβ₁₋₄₂ + CeONP, respectively. Concentrations of both Aβ and CeONP are 50 μM.

Reactive oxygen species (ROS) is the critical factor responsible for neuronal cytotoxicity induced by Aβ₁₋₄₂ and redox metal ions. The concentration of ROS in living cells was sensitively detected by the fluorescent probe with an ROS assay.¹⁵ Green fluorescence intensity is in proportion to the ROS concentration in the cells. The reduction of ROS by the CeONP was detected using the fluorescent probe DCFH in SH-SY5Y cells in the presence of Aβ₁₋₄₂ or Cu²⁺+Aβ₁₋₄₂. As shown in

Figure 4, $A\beta_{1-42}$ and Cu^{2+} - $A\beta_{1-42}$ produced obvious amount of ROS. With the addition of CeONP, green fluorescence intensity of DCFH decreased significantly indicating that CeONP can reduce the amount of ROS in cells. The results are consistent with those found in cell viability experiments to ascertain that the cellular toxicity is in line with the generation of ROS induced by $A\beta_{1-42}$ or Cu^{2+} + $A\beta_{1-42}$.⁷

To further probe the molecular mechanism for CeONP to protect against neuronal cytotoxicity from amyloid peptide and copper ions, EPR was applied. The redox active Cu^{2+} ions bound with $A\beta_{1-42}$ produce reactive oxygen species (ROS) by Fenton-type and Harber–Weiss-type reactions, resulting in oxidative stress of the cells.⁶ The generated ROS (especially hydroxyl radicals) can influence cell metabolism and also promote $A\beta_{1-42}$ aggregation. We now know that CeONP can protect from neurotoxicity of Cu^{2+} - $A\beta_{1-42}$, however, it is not clear whether CeONP reacts with redox copper ions directly, or eliminates ROS generated from $A\beta_{1-42}$ plus copper ions? In both cases, the neuronal cytotoxicity from amyloid peptide and copper ions could be reduced. As indicated in Figure 5A, treating Cu^{2+} - $A\beta_{1-42}$ with CeONP did not reduce or abolish Cu^{2+} -EPR signals, while the free radical signals induced by Cu^{2+} - $A\beta_{1-42}$ were reduced and then disappeared upon the addition of CeONP (Figure 5B). These results suggested that CeONP can be administered in an amount sufficient to abolish ROS from Cu^{2+} - $A\beta_{1-42}$ by Ce^{3+}/Ce^{4+} catalytic cycles.

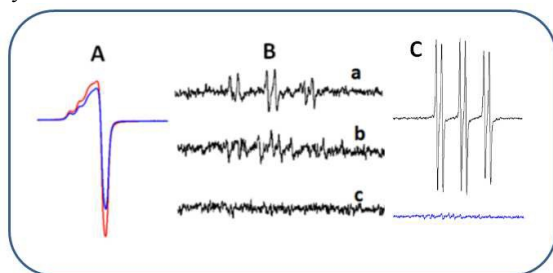


Figure 5. EPR of Cu^{2+} plus $A\beta_{1-42}$ in the presence and absence of CeONP. Panel A, Cu^{2+} ions EPR of Cu^{2+} - $A\beta_{1-42}$ (blue line) and Cu^{2+} plus $A\beta_{1-42}$ with CeONP (red line). Panel B, CeONP blocks Cu^{2+} and $A\beta_{1-42}$ -induced free radical formation [a, Cu^{2+} plus $A\beta_{1-42}$ (50 μ M); b, Cu^{2+} plus $A\beta_{1-42}$ (50 μ M) and CeONP (50 μ M); c, Cu^{2+} plus $A\beta_{1-42}$ (50 μ M) and CeONP (100 μ M)]. Panel C, CeONP abolishes radicals generated from Cu^{2+} plus $A\beta_{1-42}$ and H_2O_2 .

Cu^{2+} - $A\beta_{1-42}$ induced the production of free radicals, and this occasionally causes the formation of partially reduced oxygen forms, commonly known as ROS.¹⁹ These can be highly reactive and potentially very dangerous to neural cells, and must be scavenged by exogenous or endogenous antioxidant systems to keep their level below a critical threshold. The Ce^{3+}/Ce^{4+} switch of CeONP resembles the mechanism of redox enzymes. Reactions involving redox cycles between the Ce^{3+} and Ce^{4+} oxidation states allow CeONP to react catalytically with superoxide and hydrogen peroxide, mimicking the behaviour of two key antioxidant enzymes, SOD and catalase, potentially abating all noxious intracellular ROS via a self-regenerating mechanism.

In conclusion, morphology of TEM, MS, and Fluorescent spectroscopy of $[Ru(phen)_2dppz]^{2+}$ revealed that CeONP reduces $A\beta_{1-42}$ aggregation. Cell viability assay and fluorescence assays of ROS in living SH-SY5Y cells indicated that CeONP protects neurotoxicity of $A\beta_{1-42}$ or Cu^{2+} - $A\beta_{1-42}$ by scavenging ROS radical production via Ce^{3+}/Ce^{4+} catalytic cycles. EPR studies

demonstrated that CeONP doesn't react directly with Cu^{2+} ions, while it scavenges ROS generated from Cu^{2+} - $A\beta_{1-42}$. All these results provide valuable insights into the molecular mechanism for CeONP as a therapeutic intervention to reduce oxidative damage in Alzheimer's disease.

Acknowledgements: This work was supported partly by the National Natural Science Foundation of China (No. 21472027, No.31270869, and No. 91013001 to XT), the Ph.D. Program of the Education Ministry of China (20100071110011), the high magnetic field laboratory of Chinese Academy of Science, and Shanghai Synchrotron Radiation Facility (SSRF). We are grateful to Dr Tianming Yao and Shuo Shi from Tongji University for generously offering the $[Ru(phen)_2dppz]^{2+}$ complex.

Notes and references

- ⁷⁰ *Department of Chemistry & Institutes of Biomedical Sciences, Fudan University, Shanghai 200433, China.*
E-mail: xstan@fudan.edu.cn; Fax: +86-21-65641740; Tel: +86-21-55664475
- ⁷¹ *State Key Laboratory of Medical Neurobiology, Shanghai Medical College of Fudan University, Shanghai, China*
- ⁷² *Department of Chemistry & College Station High School, Texas A&M University, Texas 77845, USA*
- ⁷³ †Electronic Supplementary Information (ESI) available: Experimental procedures. See DOI: 10.1039/b000000x
1. X. Wang, W. Zheng, J.W. Xie, T. Wang, S.L. Wang, W.P. Teng, and Z.Y. Wang, *Mol. Neurodegener.*, 2010, **46**, 1326.
2. I. W. Hamley, *Chem. Rev.*, 2012, **112**, 5147.
3. C. Haass and D. J. Selkoe, *Cell*, 1993, **75**, 1039.
4. F. Prelli, E. M. Castano, S. G. van Duinen, G. T. Bots, W. Luyendijk and B. Frangione, *Biochem. Biophys. Res. Commun.*, 1988, **151**, 1150.
5. W. R. Markesbery, *Free. Rad. Biol. Med.*, 1997, **23**, 134.
6. P. Faller, and C. Hureau, *Dalton. Trans.*, 2009, **7**, 1080.
7. M. Li, P. Shi, J. Ren, and X. Qu, *Chem. Sci.*, 2013, **4**, 2536.
8. R. D. Robinson, J. E. Spanier, F. Zhang, S. Chan, and I. P. Herman, *J. Appl. Physiol.*, 2002, **92**, 1936.
9. F. Esch, S. Fabris, L. Zhou, T. Montini, C. Africh, P. Fornasiero, G. Comelli, and R. Rosei, *Science*, 2005, **309**, 752.
10. G. Liu, P. Men, P. L. Harris, R. K. Rolston, G. Perry and M. A. Smith, *Neurosci. Lett.*, 2006, **406**, 189.
11. G. Liu, M. R. Garrett, P. Men, X. Zhu, G. Perry and M. A. Smith, *Biochem. Biophys. Acta, Mol. Basis. Dis.*, 2005, **246**, 1741.
12. I. Y. Seong, M. Yang, J. R. Brender, V. Subramanian, K. Sun, N. E. Joo, S. Jeong, A. Ramamoorthy and N. A. Kotov, *Angew. Chem., Int. Ed.*, 2011, **50**, 5110.
13. A. Cimini, B. D'Angelo, S. Das, R. Gentile, E. Benedetti, V. Singh, A. M. Monaco, S. Santucci and S. Seal, *Acta. Biomater.*, 2012, **8**, 2056.
14. A. A. Reinke, H. Y. Seh, J.E. and Gestwicki, *Bioorg. Med. Chem. Lett.*, 2009, **19(17)**, 4952.
15. X. P. LV, W. Li, Y. Luo, D. Wang, C. Zhu, Z. X. Huang, and X. Tan, *Chem. Commun.*, 2013, **49**, 5865.
16. N. P. Cook, K. Kilpatrick, L. Segatori, and A. A. Marti, *J. Am. Chem. Soc.*, 2012, **134**, 20776.
17. N. P. Cook, V. Torres, D. Jain, and A. A. Marti, *J. Am. Chem. Soc.*, 2011, **133**, 11121.
18. Q. G. Bao, Y. Luo, X. Sun, C. Zhu, P. Li, Z. Huang, and X. Tan, *J. Biol. Chem.*, 2011, **16**, 809.
19. I. Celardo, J. Z. Pedersen, E. Traversab and L. Ghibelli, *Nanoscale*, 2011, **3**, 1411.
20. N.P. Cook, K. Kilpatrick, L. Segatori, A.A. Marti, *J. Am. Chem. Soc.*, 2012, **134**, 20776.
21. N.P. Cook, M. Ozbil, C. Katsampes, R. Prabhakar, A.A. Marti, *J. Am. Chem. Soc.*, 2013, **135**, 10810.